Magnetoelastically coupled structural, magnetic, and superconducting order parameters in $BaFe_2(As_{1-x}P_x)_2$

H.-H. Kuo,[1,2,*] James G. Analytis,[1,3,*] J.-H. Chu,[1,3] R. M. Fernandes,[4,5] J. Schmalian,[6] and I. R. Fisher[1,3]

[1]*Stanford Institute for Materials and Energy Sciences, SLAC National Accelerator Laboratory, 2575 Sand Hill Road, Menlo Park, California 94025, USA*

[2]*Geballe Laboratory for Advanced Materials and Department of Materials Science and Engineering, Stanford University, USA*

[3]*Geballe Laboratory for Advanced Materials and Department of Applied Physics, Stanford University, USA*

[4]*Department of Physics, Columbia University, New York, New York 10027, USA*

[5]*Theoretical Division, Los Alamos National Laboratory, Los Alamos, New Mexico 87545, USA*

[6]*Institute for Theory of Condensed Matter Physics and Center for Functional Nanostructures, Karlsruhe Institute of Technology, Karlsruhe 76131, Germany*

(Received 2 May 2012; revised manuscript received 7 August 2012; published 4 October 2012)

We measure the transport properties of mechanically strained single crystals of $BaFe_2(As_{1-x}P_x)_2$ over a wide range of x. The Néel transition is extremely sensitive to stress and this sensitivity increases as optimal doping is approached (doping with the highest superconducting T_c), even though the magnetic transition itself is strongly suppressed. Furthermore, we observe significant changes in the superconducting transition temperature with applied strain, which mirror changes in the composition x. These experiments are a direct illustration of the intimate coupling between different degrees of freedom in iron-based superconductors, revealing the importance of magnetoelastic coupling to the magnetic and superconducting transition temperatures.

DOI: 10.1103/PhysRevB.86.134507 PACS number(s): 74.70.−b, 71.18.+y, 74.25.Bt, 74.25.Jb

I. INTRODUCTION

Materials that exhibit unconventional superconductivity are almost always in the proximity of alternative, often magnetic ground states. Each ground state is characterized by a broken symmetry and an associated order parameter which acquires a finite value at the critical temperature, indicating the transition has occurred. The iron-based superconductors fall within a broad family of correlated electron materials which are related to antiferromagnetism, joining the cuprate, heavy-fermion, and layered organic superconductors. The relationship of the magnetic, structural, and other (sometimes unknown) order parameters, and particularly how these conspire to give rise to high superconducting critical temperatures T_c, is one of the most important experimental challenges in understanding the mechanism behind high-temperature superconductivity.

In the present work, we reveal the intimate relationship between different broken-symmetry ground states in the $BaFe_2As_2$ superconducting family of iron pnictides. When left chemically unmolested, these materials are characterized by a high-temperature phase that is tetragonal (Tet) and paramagnetic, transitioning at ∼138 K to an orthorhombic (Ort), collinear antiferromagnet (AFM).[1] In this case, the structural transition breaks tetragonal symmetry ($C_4 \rightarrow C_2$), and the shear strain $u_{xy} \equiv \partial_y u_x + \partial_x u_y$ plays the role of the order parameter. The magnetic order breaks both spin-rotational and tetragonal symmetry, characterized by an order parameter corresponding to the staggered sublattice magnetization $\mathbf{M}_i$ where $i = 1,2$ refers to the magnetization of each sublattice.[2–4] When $BaFe_2As_2$ is electron, hole, or isovalently "doped,"[1,5–7] these transitions are suppressed and superconductivity (SC) emerges, with optimal T_c appearing when magnetism is completely absent, indicating that AFM and SC order parameters compete. While for electron-doped materials the structural (T_S) and magnetic (T_N) transitions separate[5,8,9] with $T_S > T_N$, in the present isovalently substituted $BaFe_2(As_{1-x}P_x)_2$ materials, no such splitting is observed at any composition.

Several theoretical descriptions have attempted to explain the coupling between the structural and magnetic transition, based on pure ferroelastic phenomenology or inclusion of a nematic order parameter.[2,3,10] Despite the different approaches of each of the works, all of them highlight the importance of the magnetoelastic coupling, which can cause the two transitions to split or to occur simultaneously. Here, we investigate the role of the magnetoelastic coupling by studying the thermodynamic response of the material $BaFe_2(As_{1-x}P_x)_2$ to a small mechanical strain applied along the tetragonal $[110]_T$ direction, or equivalently the orthorhombic b axis when $T < T_N$. We find that a small shear stress σ applied in the $[110]_T$ direction see top Fig. 3(a) can significantly alter the Néel transition T_N and superconducting T_c, in a manner akin to changing x. Surprisingly, even though the magnetism is almost completely suppressed at optimal doping, the effect on the magnetic transition grows, suggesting that magnetoelastic fluctuations substantially increase near optimal T_c.

II. EXPERIMENTAL METHODS

The growth of single crystals of $BaFe_2(As_{1-x}P_x)_2$ is described elsewhere.[11] It is worth noting however that the quality of the crystals can be improved by annealing within the growth for a week at 900 °C. Samples were mechanically strained along either the $[100]_T$, $[001]_T$, or $[110]_T$ direction using a custom built mechanical device described in Ref. 12, as illustrated in the top of Fig. 3. A cantilever was pressed against the sample by adjusting a turnable screw, applying <10 MPa, determined by measuring the cantilever deflection.[12] To ensure the same stress was applied to each composition x, the samples were cut to have similar dimensions (∼300×200×80 μm^3)

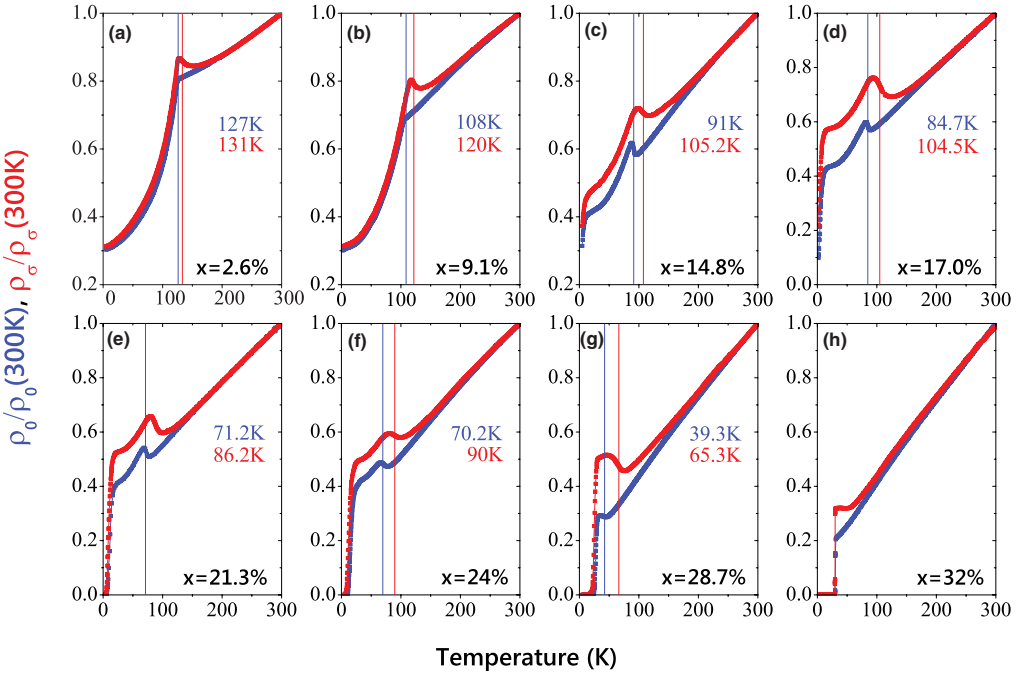

FIG. 1. (Color online) Temperature dependence of the normalized resistivity, $\rho/\rho(300\ \mathrm{K})$, for unstressed (blue) and uniaxially stressed along $[110]_T$ (red) $BaFe_2(As_{1-x}P_x)_2$ crystals with $x = 2.6\%$ to $x = 32\%$. T_N determined from $d\rho/dT$ are labeled and denoted by vertical lines with corresponding colors (see Appendix A for details).

and the cantilever screw adjusted by the same amount. Further reduction to the errors associated with differences in stress was achieved by repeating the experiments on at least 3 distinct samples from each batch. This gives us confidence that we are able to apply a similar stress to all samples and hence that the changes we detect between samples at distinct P content x are in fact intrinsic. This study is distinct from our earlier investigations of the transport anisotropy, which is a nonequilibrium property, whereas we presently focus on the effect of mechanical strain on the temperature of the phase transitions themselves.

III. RESULTS

Figures 1(a)–1(h) illustrate the main experimental data. In each panel we show the normalized resistivity vs temperature for an unstressed (blue) and stressed (red) crystal at a given doping, where the stress has been applied along the $[110]_T$. The vertical lines denote the assigned Néel transitions for each curve which have been determined by the maximum negative value of the resistivity derivative (Appendix A). Note that in contrast to electron-doped materials where two anomalies are observed in $d\rho/dT$ in the *unstrained* samples, we only observe one in $BaFe_2(As_{1-x}P_x)_2$, indicating that $T_N \approx T_S$ for all x.[5] This may suggest that the magneto-elastic coupling in these materials is perhaps larger,[3,10] though we point out that other studies have observed split transitions in these compounds.[6] In the presence of mechanical strain, the structural transition will naturally broaden to higher temperatures, but by continuity, the anomaly seen in the data of mechanically strained samples must be associated with the magnetic order.

In all the samples we studied, $\Delta T_N = T_N(\sigma) - T_N(\sigma = 0) > 0$, where σ indicates the mechanical strain field (the stress). Intriguingly, for the unstressed optimally superconducting $x = 32\%$ sample [blue curve in Fig. 1(h)] there is no detectable magnetic transition, but after application of stress a distinct minimum arises at 45 K, almost identical to the minimum seen in the unstressed samples at lower doping [consider blue curve in Fig. 1 (g)]. It appears that the magnetic transition has been summoned from beneath the superconducting dome by the application of mechanical strain. Even though the magnetic order itself vanishes, the strong magnetoelastic coupling as well as magnetic and elastic fluctuations remain.

In Fig. 2 we show the same data presented in Fig. 1, but focus around the superconducting critical temperature at each composition. In this case T_c is defined as the midpoint in the superconducting transition. Even though the transition becomes

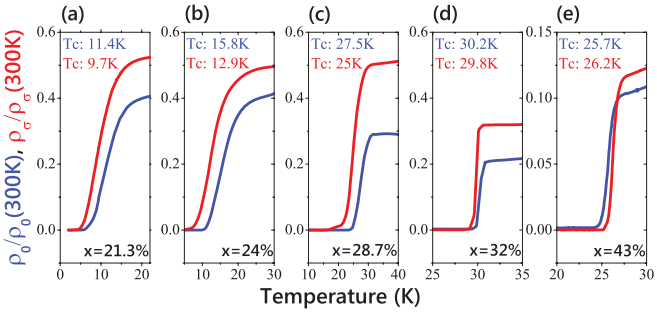

FIG. 2. (Color online) Expanded view of the data shown in Fig. 1 around T_c for $x = 21.3\%$ to $x = 32\%$ [(a) to (d), underdoped] and $x = 21.3\ \%$ [(e), overdoped]. Red and blue curves correspond to the normalized resistivity of unstressed and uniaxially stressed (along $[110]_T$), respectively. For underdoped samples, $\Delta T_c > 0$; for overdoped samples, $\Delta T_c < 0$.

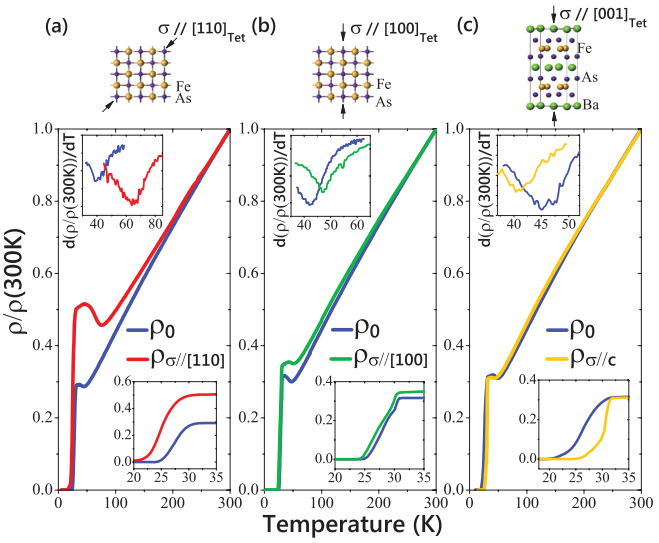

FIG. 3. (Color online) Temperature dependence of normalized in-plane resistivity $\rho/\rho(300\ \mathrm{K})$, for unstressed crystals and (a) uniaxially stressed along $[110]_T$ (red), (b) uniaxially stressed along $[100]_T$ (green), and (c) uniaxially stressed along the crystal c axis (yellow) $BaFe_2(As_{1-x}P_x)_2$ crystals with $x = 28.7\%$. The upper inserts show $d\rho/dT$ vs T of each crystal around T_N with corresponding colors. (a) $\Delta T_N \sim 27$ K, (b) $\Delta T_N \sim 5$ K, (c) $\Delta T_N \sim -5$ K. The lower intercepts are magnified plots of ρ vs T around T_c. (a) $\Delta T_c \sim -2.5$ K, (b) $\Delta T_c \sim -0.3$ K, (c) $\Delta T_c \sim 4$ K.

broader with the application of strain, the superconducting T_c nevertheless can be seen to *decrease* as stress is applied until compositions beyond optimal x, where we observe T_c to increase [Fig. 2(e) illustrates that $\Delta T_c = T_c(\sigma) - T_c(\sigma = 0)$ switches sign beyond optimal x]. The effect of stress on T_N and T_c can be demonstrated to be intrinsic by applying a systematically increasing amount of stress (Appendix B). These data are suggestive that the application of shear stress has a similar effect to that of decreasing x across the phase diagram.

To ensure that this effect is indeed intrinsic to pressure along one of the orthorhombic axes, we also apply pressure along $[100]_T$, shown for comparison on two samples from the same batch in Figs. 3(a) and 3(b). Mechanical strain in this direction results in small changes in both magnetic and superconducting transitions. We furthermore apply pressure in the interlayer c direction [Fig. 3(c)] and found the opposite behavior whereby $\Delta T_N < 0$ and $\Delta T_c > 0$. This suggests that the ratio c/b, whether directly or indirectly, likely plays a role in the superconducting mechanism.

IV. DISCUSSION

In Fig. 4(a) we plot the change in the Néel temperature ΔT_N as a function of doping for nominally the same stress at each doping. Surprisingly, even though the magnetic and the structural transitions are suppressed as a function of doping, the amount that T_N can be changed by stress monotonically *increases* with P content, within our error bars. This is in contrast to the value of the resistivity anisotropy itself, which is highly nonmonotonic with doping (Appendix C). If we also include data of $T_N(\sigma)$ at $x = 32\%$, ΔT_N appears to have the

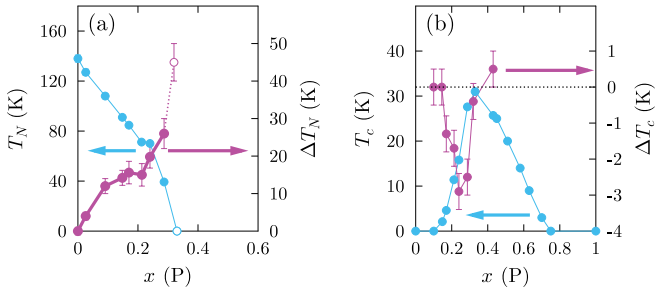

FIG. 4. (Color online) (a) $T_N(\sigma = 0)$ (blue, left axis) and ΔT_N (pink, right axis) vs P concentration x. Points at optimal doping are distinguished as open circles because they rely on the assumption that $T_N(\sigma = 0) = 0$. (b) $T_c(\sigma = 0)$ (blue, left axis) and ΔT_c (pink, right axis) vs P concentration x. Dotted black line indicates $\Delta T_c = 0$. In both (a) and (b) the source of error is predominantly related to our ability to accurately determine minima in the resistivity derivative about the Néel and superconducting transitions. The size of the effect we see on each of these transitions is confirmed on multiple samples.

largest response at optimal doping, as shown in Fig. 4(a). This large enhancement of ΔT_N implies an enhanced susceptibility of the AFM ground state to shear stress.

In Fig. 4(b), we illustrate the equivalent plot of changes in the superconducting critical temperature ΔT_c as a function of doping for nominally the same strain. ΔT_c, unlike ΔT_N, is not monotonic with x. Comparing the dependence with the evolution of the *unstressed* superconducting transition with x, it appears that the magnitude of ΔT_c is largest where the $T_c(x)$ dome is steepest and small otherwise; mathematically ΔT_c increases as $-dT_c/dx$. Indeed, considering Fig. 4(a) a very similar relationship likely applies to the magnetic transition, so that ΔT_N increases as $-dT_N/dx$. As T_N is enhanced, there are likely fewer electrons available to participate in superconductivity,[13–15] and so the fact that T_c decreases with applied stress in the underdoped region is not surprising, since T_N increases. However, we note than an unstrained sample with a given T_N has always a T_c that is lower than a strained sample with the same T_N; i.e., $T_c(T_N,0) < T_c(T_N,\sigma)$. Therefore, there is an intrinsic effect of stress on T_c, beyond the indirect effect due to the competition between AFM and SC.

We employ a Ginzburg-Landau (GL) approach to obtain further insight into our observations. The GL model has been applied to the ferro-pnictides by several authors already to describe the coupling between structure and magnetism.[2–4,16–18] From symmetry considerations, the coupling between magnetic and elastic degrees of freedom enters the free energy via

$$F_{ME} = g\,(\mathbf{M}_1 \cdot \mathbf{M}_2)\,u_{xy}, \tag{1}$$

where g is the magnetoelastic coupling. In order to describe the present experiment, we need to add also the term $-\sigma u_{xy}$, where σ is the applied mechanical stress. If one assumes that the structural and magnetic transitions occur independently, the coupling (1) effectively ties them together.[3] Alternatively, it has been proposed that the structural transition is a secondary consequence of an underlying electronic order dubbed nematic.[12] In this case, an independent order parameter $\eta \propto \langle \mathbf{M}_1 \cdot \mathbf{M}_2 \rangle$ condenses and triggers the structural transition

via the coupling (1). Within this approach, the elastic degrees of freedom are not intrinsically soft and can be integrated out from the partition function (see Appendix D for more details), yielding the contribution to the free energy $\propto \frac{g\sigma}{C_s^0}(\mathbf{M}_1 \cdot \mathbf{M}_2)$, where C_s^0 is the bare elastic shear constant (see also Refs. 19 and 20). This term shows that the mechanical stress is converted into a conjugate field $\sigma g/C_s^0$ to the electronic order parameter η. Furthermore, it also changes the magnetic part of the free energy, resulting in an increase of the magnetic transition temperature $T_N(\sigma \neq 0) > T_N(\sigma = 0)$.

As x approaches optimal compositions, we observe that the magnetoelastic response is enhanced, which suggests that g/C_s^0 increases substantially and is strongest at optimal doping. In contrast, our previous mechanical strain studies on $Ba(Fe_{1-x}Co_x)_2As_2$ did not show significant changes in T_N, and changes have only been observed for pressures $\sim 5\times$ those used here,[21] though a recent neutron study in the parent compound could detect changes in T_N at much smaller pressures.[22] Nevertheless, as a function of Co doping the difference between T_N and T_S grows,[5,8] which could be interpreted in terms of a decreasing g.[3,10] Furthermore, even though the lattice softens as a function of temperature, the average value of C_s^0 in fact increases as a function of Co doping.[4,23] Here, in contrast, the effect of stress on T_N is strongly enhanced as x increases in $BaFe_2(As_{1-x}P_x)_2$, suggesting that either g becomes larger or C_s^0 smaller, or both. Another possibility is that, near optimal doping, where there is no structural or magnetic transitions, the nematic susceptibility χ_{nem} is enhanced, providing an additional contribution that enhances the "conjugate field" $\frac{g\sigma}{C_s^0}\chi_{\text{nem}}(\mathbf{M}_1 \cdot \mathbf{M}_2)$ and, consequently, ΔT_N (see Appendix D). Interestingly, experiments have indicated that magnetic fluctuations are critical at optimally doped $BaFe_2(As_{1-x}P_x)_2$,[6] which could suggest a close connection between nematic and magnetic fluctuations in these compounds.[4,17]

Furthermore, magnetic fluctuations enhance the repulsive interband pairing interaction that can lead to an unconventional superconducting state.[24] Nematic fluctuations, on the other hand, give rise to an attractive intraband pairing interaction, which can potentially enhance the transition temperature of the unconventional SC phase.[25]

Previous x-ray studies on $Ba(Fe_{1-x}Co_x)_2As_2$ showed that u_{xy} is strongly suppressed below T_c,[26] indicating that the SC and orthorhombic phases compete. One would then expect that by applying stress and inducing a nonzero u_{xy}, T_c would decrease. However, our observations that $T_c(\sigma) > T_c(0)$ in the overdoped region and $T_c(T_N,\sigma) > T_c(T_N,0)$ in the underdoped region suggest that the applied stress may actually lead to an intrinsic increase of T_c. To understand the effect of mechanical stress on superconductivity, we can compare to the case of high-T_c copper-oxide-based materials.[27–29] Though the effects vary between different compounds, Hardy *et al.* proposed a unified picture of the influence of uniaxial strain (excluding YBCO), whereby changes in T_c could be accounted for by changes in the ratio c/a.[29] In the present study, c/b will always increase when stress is applied along $[110]_T$, and by a smaller amount when applied along $[100]_T$, but will decrease when applied along c (see Fig. 3). The changes we are able to invoke on the underdoped samples follow this trend, so that qualitatively ΔT_c increases with $\Delta(c/b)$. However, one cannot say whether it is the lattice parameters alone, their ratio, or some other systematically adjusted internal parameter which is most important (such as the As-Fe-As bond angle). Direct structural measurements as a function of mechanical strain are required to answer this question.

V. CONCLUSIONS

In conclusion, we have found a strongly enhanced magnetoelastic response in $BaFe_2(As_{1-x}P_x)_2$ as x approaches optimal doping, which may be related to the superconducting mechanism itself. We also find that mechanical strain can directly couple to the superconducting order parameter in a manner that is similar to decreasing the P concentration x. These experiments are therefore a direct illustration of the subtle coupling between different degrees of freedom in $BaFe_2(As_{1-x}P_x)_2$.

ACKNOWLEDGMENTS

R.M.F. acknowledges support of NSF Partnerships for International Research and Education (PIRE) Program No. OISE-0968226. H.H.K., J.G.A., J.H.C., and I.R.F. acknowledge support of the US DOE, Office of Basic Energy Sciences, under Contract No. DE-AC02-76SF00515.

APPENDIX A: DETERMINATION OF THE NÉEL TEMPERATURE FROM THE RESISTIVITY DERIVATIVE

The Fermi surface reconstruction associated with the Néel order at T_N appears as a pronounced minimum in the derivative with respect to temperature. After applying strain, we observe an increase in T_N, as shown in Fig. 5. Blue and red represent unstressed and uniaxially stressed (along $[110]_T$) $BaFe_2(As_{1-x}P_x)_2$ single crystals, respectively. Even though the stress broadens the transition, the increase in T_N can be easily resolved.

APPENDIX B: SYSTEMATIC RESPONSE OF T_N TO PRESSURE

Although we cannot determine the absolute value of stress applied, we can nevertheless tune the amount of pressure applied by gradually tightening the screw on the device. As a typical example, two samples of $BaFe_2(As_{1-x}P_x)_2$, $x = 23.1\%$ and $x = 28.7\%$, are shown in Fig. 6. Each sample was measured with a different amount of stress applied along $[110]_T$. $|\Delta T_N|$ and $|\Delta T_c|$ increase with increasing stress.

APPENDIX C: RESISTIVITY ANISOTROPY

The in-plane resistivity anisotropy of $BaFe_2(As_{1-x}P_x)_2$ was obtained by measuring the resistivity of mechanically detwined crystals as described elsewhere[9] (see Fig. 7). Clearly, the resistivity anisotropy has a highly nonmonotonic dependence on doping. This is in contrast to the trend of the response of T_N at constant stress as a function of doping, which is a monotonic increase with the concentration x, as shown in Fig. 4.

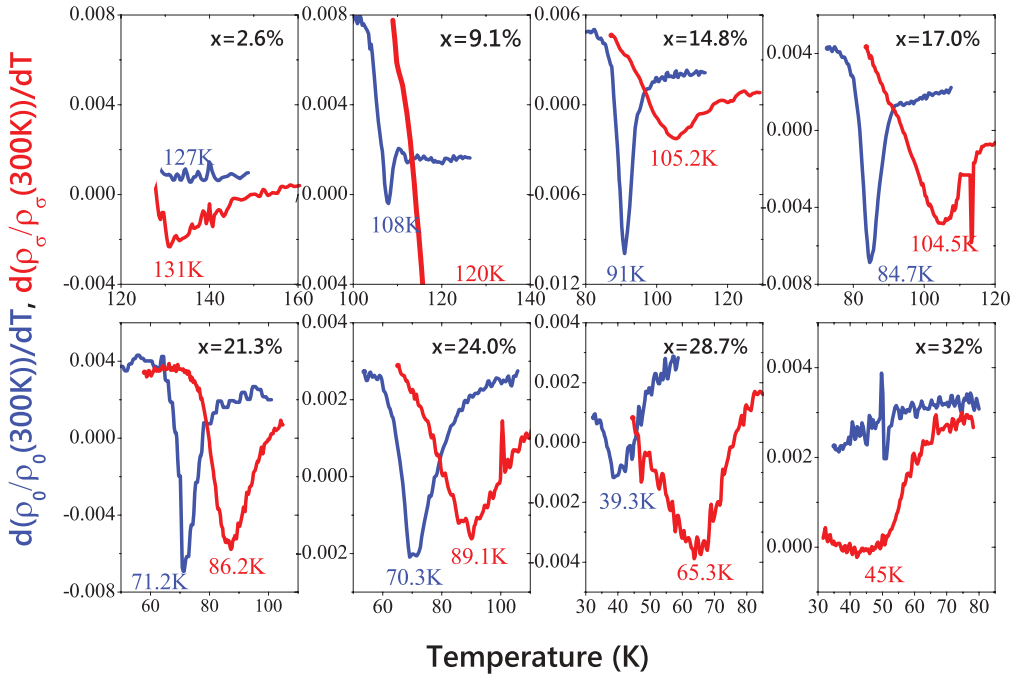

FIG. 5. (Color online) Derivative of normalized resistivity with respect to temperature, $\frac{d}{dT}\rho/\rho(300\text{ K})$, for unstressed (blue) and uniaxially stressed along $[110]_T$ (red) $BaFe_2(As_{1-x}P_x)_2$ crystals with $x = 2.6\%$ to $x = 32\%$. The minimum in $d\rho/dT$ is shown in corresponding color, and is interpreted as the Néel temperature T_N.

APPENDIX D: GINZBURG-LANDAU ANALYSIS

To understand how the different degrees of freedom affect T_N in mechanically stressed samples, we use a phenomenological Ginzburg-Landau model for the magnetic, nematic, and elastic degrees of freedom. For the magnetic part, we have

$$F_{\text{mag}} = \frac{r_0}{2}\left(M_1^2 + M_2^2\right) + \frac{u}{8}\left(M_1^2 + M_2^2\right)^2 - \frac{\lambda}{2}(\mathbf{M}_1 \cdot \mathbf{M}_2)^2 \tag{D1}$$

where $\mathbf{M}_1$ and $\mathbf{M}_2$ are the staggered magnetization of the two interpenetrating Néel sublattices. Here, we defined $r_0 = a(T - T_{N,0})$, with $T_{N,0}$ denoting the mean-field magnetic transition temperature. The coupling constants satisfy $u > 0$

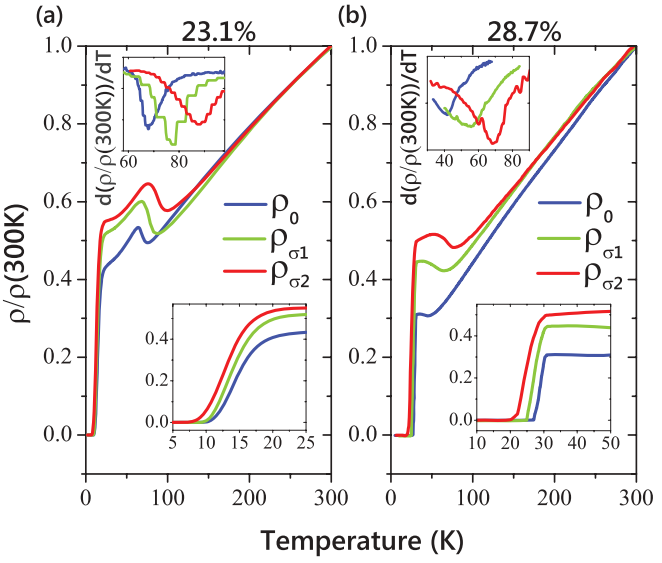

FIG. 6. (Color online) Temperature dependence of normalized resistivity of $BaFe_2(As_{1-x}P_x)_2$, $x = 23.1\%$ and $x = 28.7\%$, at three systematically increased amounts of stress. The normalized resistivity ρ_i with $i = \{0,\sigma 1,\sigma 2\}$ stand for unstressed (blue), intermediately stressed (green), and highly stressed (red), respectively. The upper inserts show $d\rho_i/dT$ vs T near T_N, and the lower inserts are expanded plots of ρ_i near T_c.

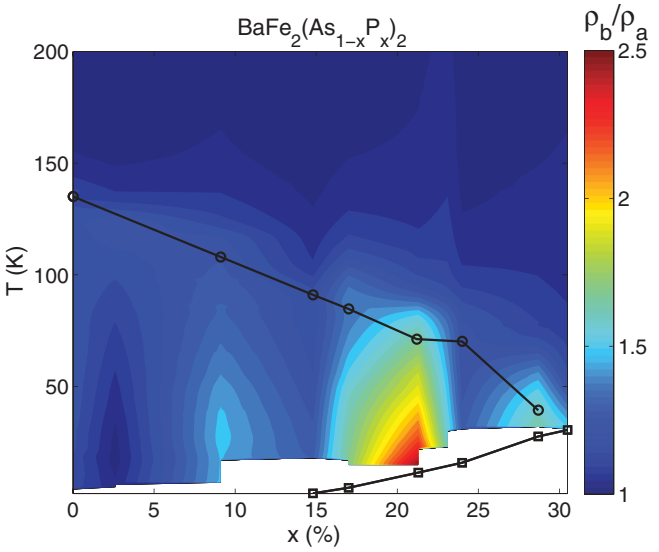

FIG. 7. (Color online) In-plane resistivity anisotropy ρ_a/ρ_b as a function of temperature and doping for $BaFe_2(As_{1-x}P_x)_2$. The color scale has been obtained by a linear interpolation between adjacent data points. Black circles and squares indicate T_s/T_N and T_c, respectively.

and $\lambda > 0$, such that in the free-energy minimum $\mathbf{M}_1$ and $\mathbf{M}_2$ are either parallel or antiparallel, corresponding to the two possible magnetic stripe configurations with ordering vectors $(\pi,0)$ and $(0,\pi)$ in the 1-Fe unit cell Brillouin zone. It is convenient to introduce the order parameters of these two magnetic stripe states $\mathbf{\Delta}_1$ and $\mathbf{\Delta}_2$, such that $\mathbf{\Delta}_1 = (\mathbf{M}_1 + \mathbf{M}_2)/2$ and $\mathbf{\Delta}_2 = (\mathbf{M}_1 - \mathbf{M}_2)/2$. Notice that $M_1^2 + M_2^2 = 2(\Delta_1^2 + \Delta_2^2)$ and $\mathbf{M}_1 \cdot \mathbf{M}_2 = \Delta_1^2 - \Delta_2^2$.

We now consider the nematic part in a phenomenological way. The nematic order parameter φ breaks the tetragonal symmetry of the lattice. At high enough temperatures (compared to the structural transition temperature), such as those for the optimally doped compounds, we consider the free energy expansion only up to second order in the nematic order parameter:

$$F_{\text{nem}} = \tfrac{1}{2}\left(\chi_{\text{nem}}^{(0)}\right)^{-1}\varphi^2 - \kappa\varphi\left(\Delta_1^2 - \Delta_2^2\right), \tag{D2}$$

where κ is the coupling between nematic and magnetic degrees of freedom, and $\chi_{\text{nem}}^{(0)}$ is the static nematic susceptibility. For the elastic part, we consider a harmonic lattice

$$F_{el} = \frac{C_s^0}{2}u_{xy}^2 - g u_{xy}\varphi - \sigma u_{xy}, \tag{D3}$$

where g is the magnetoelastic coupling, C_s^0 is the bare shear modulus, and σ is the applied stress.

To study how $T_{N,0}$ changes as function of σ, we first integrate out the elastic degrees of freedom from the partition function

$$\int du_{xy}\, e^{-(C_s^0/2)u_{xy}^2 + u_{xy}(g\varphi+\sigma)} \propto \exp\left[\frac{(g\varphi+\sigma)^2}{2C_s^0}\right]. \tag{D4}$$

Substituting in Eq. (D2), the nematic free energy becomes

$$F_{\text{nem}} = \frac{\chi_{\text{nem}}^{-1}}{2}\varphi^2 - \varphi\left[\kappa\left(\Delta_1^2 - \Delta_2^2\right) + \frac{g\sigma}{C_s^0}\right], \tag{D5}$$

where we defined the renormalized nematic susceptibility $\chi_{\text{nem}}^{-1} = (\chi_{\text{nem}}^{(0)})^{-1} - g^2/2C_s^0$. If we consider the regime where the nematic free energy can be approximated by the quadratic expansion (D2), we can also integrate out the nematic degrees of freedom, obtaining

$$\int d\varphi\, \exp\left\{-\frac{\chi_{\text{nem}}^{-1}}{2}\varphi^2 + \varphi\left[\kappa\left(\Delta_1^2 - \Delta_2^2\right) + \frac{g\sigma}{C_s^0}\right]\right\} \propto \exp\left[\frac{\left(\kappa\left(\Delta_1^2 - \Delta_2^2\right) + \frac{g\sigma}{C_s^0}\right)^2}{2\chi_{\text{nem}}^{-1}}\right]. \tag{D6}$$

Substituting in Eq. (D1), the magnetic free energy becomes

$$\begin{aligned} F_{\text{mag}} = {} & r_0\left(\Delta_1^2 + \Delta_2^2\right) + \frac{u}{2}\left(\Delta_1^2 + \Delta_2^2\right)^2 \\ & - \frac{1}{2}\left(\lambda + \frac{\kappa^2}{\tilde{\chi}_{\text{nem}}^{-1}}\right)\left(\Delta_1^2 - \Delta_2^2\right)^2 \\ & - \frac{g\kappa\sigma}{\chi_{\text{nem}}^{-1}C_s^0}\left(\Delta_1^2 - \Delta_2^2\right). \end{aligned} \tag{D7}$$

The last term acts as a conjugate field and breaks the tetragonal symmetry, selecting the magnetic stripe configuration corresponding to the Δ_1 order parameter [ordering vector $(\pi,0)$]. Since $r_0 = a(T - T_{N,0})$, the magnetic transition temperature is given by

$$T_N = T_{N,0} + \left(\frac{g\kappa\chi_{\text{nem}}}{aC_s^0}\right)\sigma. \tag{D8}$$

Hence, the increase in T_N is proportional to the applied strain σ. The enhanced response at optimal doping can be due to one (or a combination) of the following features: an intrinsic softening of the lattice (i.e., decrease of C_s^0), an enhancement to the magnetoelastic coupling (i.e., increase of g and/or κ), and an enhancement of nematic fluctuations (i.e., increase of χ_{nem}). A similar enhancement in T_N is also expected even in the absence of a nematic order parameter, as pointed out recently by Cano and Paul.[19]

*These authors contributed equally to this work. Correspondence should be addressed to analytis@slac.stanford.edu

[1] M. Rotter, C. Hieke, and D. Johrendt, Phys. Rev. B **82**, 014513 (2010).
[2] V. Barzykin and L. P. Gor'kov, Phys. Rev. B **79**, 134510 (2009).
[3] A. Cano, M. Civelli, I. Eremin, and I. Paul, Phys. Rev. B **82**, 020408 (2010).
[4] R. M. Fernandes *et al.*, Phys. Rev. Lett. **105**, 157003 (2010).
[5] J. H. Chu, J. G. Analytis, C. Kucharczyk, and I. R. Fisher, Phys. Rev. B **79**, 014506 (2009).
[6] S. Kasahara *et al.*, Phys. Rev. B **81**, 184519 (2010).
[7] A. Thaler *et al.*, Phys. Rev. B **82**, 014534 (2010).
[8] C. R. Rotundu and R. J. Birgeneau, Phys. Rev. B **84**, 092501 (2011).
[9] H. Kuo *et al.*, Phys. Rev. B **84**, 054540 (2011).
[10] R. M. Fernandes, A. V. Chubukov, J. Knolle, I. Eremin, and J. Schmalian, Phys. Rev. B **85**, 024534 (2012).
[11] J. G. Analytis, J. H. Chu, R. D. McDonald, S. C. Riggs, and I. R. Fisher, Phys. Rev. Lett. **105**, 207004 (2010).
[12] J. H. Chu *et al.*, Science **329**, 824 (2010).
[13] A. B. Vorontsov, M. G. Vavilov, and A. V. Chubukov, Phys. Rev. B **79**, 060508(R) (2009).
[14] R. M. Fernandes and J. Schmalian, Phys. Rev. B **82**, 014521 (2010).
[15] A. Jesche, C. Krellner, M. de Souza, M. Lang, and C. Geibel, Phys. Rev. B **81**, 134525 (2010).
[16] I. I. Mazin and M. D. Johannes, Nat. Phys. **5**, 141 (2009).
[17] I. Paul, Phys. Rev. Lett. **107**, 047004 (2011).
[18] M. G. Kim *et al.*, Phys. Rev. B **83**, 134522 (2011).
[19] A. Cano and I. Paul, Phys. Rev. B **85**, 155133 (2012).
[20] J. Hu, C. Setty, and S. Kivelson, Phys. Rev. B **85**, 100507 (2012).
[21] T. Liang *et al.*, J. Phys. Chem. Solids **72**, 418 (2011).
[22] C. Dhital *et al.*, Phys. Rev. Lett. **108**, 087001 (2012).
[23] M. Yoshizawa *et al.*, J. Phys. Soc. Jpn. **81**, 024604 (2012).

[24]I. I. Mazin, D. J. Singh, M. D. Johannes, and M. H. Du, Phys. Rev. Lett. **101**, 057003 (2008).
[25]R. Fernandes and J. Schmalian, Supercond. Sci. Technol. **25**, 084005 (2012).
[26]S. Nandi *et al*., Phys. Rev. Lett. **104**, 057006 (2010).
[27]C. Meingast, A. Junod, and E. Walker, Physica C **272**, 106 (1996).
[28]J. Locquet *et al*., Nature (London) **394**, 453 (1998).
[29]F. Hardy *et al*., Phys. Rev. Lett. **105**, 167002 (2010).